Free-Volume Extended Defects in Structurally Modified Ge-Ga-S/Se Glasses

Halyna Klym, Laurent Calvez, Anatoli I. Popov

Free-volume extended defects in structurally-modified Ge-Ga-S/Se glasses

Halyna Klym[*], *Laurent Calvez, Anatoli I. Popov*

H. Klym

Lviv Polytechnic National University, 12 Bandera Str., 79013 Lviv, Ukraine

*E-mail: klymha@yahoo.com, halyna.i.klym@lpnu.ua

L. Calvez

Equipe Verres et et Céramiques, UMR-CNRS 6226, Institute des Sciences chimiques de Rennes, Université de Rennes 1, 35042 Rennes Cedex, France

A.I. Popov

Institute for Solid State Physics, University of Latvia, Kengaraga 8, LV-1063 Riga, Latvia

Keywords: defect-related free volumes, chalcogenide glasses, positron annihilation, shrinkage, expansion

Transformation of free-volume extended defects in selected chalcogenide glasses caused by thermal annealing for 10, 25 and 50 h were studied. For $80GeSe_2$-$20Ga_2Se_3$ as well as for GeS_2-Ga_2S_3 glasses with different GeS_2 and Ga_2S_3 contents ($80GeS_2$–$20Ga_2S_3$, $82GeS_2$–$18Ga_2S_3$, $84GeS_2$–$16Ga_2S_3$) positron annihilation lifetime spectroscopy and Doppler broadening of annihilation radiation methods were applied. By analyzing the positron annihilation lifetime spectra decomposed into two components, it is shown that the observed changes in the second defect-related component for the $80GeSe_2$-$20Ga_2Se_3$ glasses confirms the agglomeration of free volumes in the initial stage of annealing (10 h) with further fragmentation (25 h) and shrinkage (50 h). Increased content of Ge-related sub-system in the GeS_2-Ga_2S_3-based glasses results in the agglomeration of free-volume defects in the $82GeS_2$–$18Ga_2S_3$ glasses with their further expansion in the $84GeS_2$-$16Ga_2S_3$ matrix.

This article has been accepted for publication and undergone full peer review but has not been through the copyediting, typesetting, pagination and proofreading process, which may lead to differences between this version and the Version of Record. Please cite this article as doi: 10.1002/pssb.202100472

1. Introduction

It is known that chalcogenide glasses (ChG) of Ge-Ga-S/Se systems have prospects for practical applications as optical modulators, fiber-optic amplifiers in the IR range, laser host materials, etc. [1-7]. Therefore, research of such materials is actively performed, in particular, studies of different atomistic imperfections such as free-volume extended defects like vacancies, clusters, voids, nanopores, cracks etc. [8,9]. These structural inhomogeneities have influence of the functional properties of ChG. Most researches focus on the study of structural [10-13], optical [14,15] and thermo-mechanical [16-19] properties of glasses. Nearest atomic arrangement in materials is studied with a variety of experimental measuring techniques including vibration and Raman scattering spectroscopy, XRD, SEM, XPS and other [20-23]. However, the selection of probes available to study defect-related free volumes is rather limited, especially at sub-nanometer scale. One of the best techniques capable to probe the finest free volumes is the positron annihilation lifetime (PAL) spectroscopy, the method grounded on physical phenomena of positron-electron interaction in a matter [24-26]. It is frequently used to identify spatial heterogeneities in crystals (dislocations, vacancy-like clusters and agglomerates etc.) [26,27], evolution of free volumes in organic polymers (size and number of open-volume holes, inner pores) [28,29], light metallic alloys (cracks, bubbles, etc.) [30], zeolites [31], gels [32], thick films [33], ceramics [34] but less commonly for network glasses.

On top of that, the positron annihilation technique in the measuring mode of Doppler broadening of annihilation radiation (DBAR) allows additional identification of dominant positron trapping sites in the tested objects. So, the combined PAL-DBAR measurements are expected to be useful to study defect-related void structure of solids affected by different structural inhomogeneities [35,36].

The PAL study of ChG in the Ge-Ga-S/Se-CsCl systems exposed by additional influence and changes of compositions were investigated in this work using two- and three-component fitting procedure of decomposition of PAL spectra [37-41]. In addition, we studied the influences of thermal annealing and composition of Ge-Ga-S/Se glasses on their microstructural properties, phase composition and optical properties [40,41]. The goal of this work is to study the evolution of defect-related extended free volumes in the $80GeSe_2$–$20Ga_2Se_3$ ChG caused by thermal annealing as well as in the GeS_2–Ga_2S_3 glasses with

different amount of GeS_2 and GaS_3 ($80GeS_2–20Ga_2S_3$, $82GeS_2–18Ga_2S_3$, $84GeS_2–16Ga_2S_3$ glasses) using combined PAL and DBAR measuring tools.

2. Experimental

ChG of GeS_2-Ga_2S_3 and $GeSe_2$-Ga_2Se_3 compositions were prepared from melting mixture of highly pure raw materials (Ge, Ga, and S/Se: 99.999%) in the sealed silica ampoule kept under 10^{-6} Pa vacuum detailed described elsewhere [40,41]. The thermal annealing of the $80GeSe_2$-$20Ga_2Se_3$ ChG was performed at 380 ^oC for 10 h, 25 h and 50 h. The densities ρ were 4.352, 4.401, 4.472 and 4.454 g/cm^3 for non-annealed $80GeSe_2$-$20Ga_2Se_3$ glasses and annealed for 10, 25 and 50 h, respectively. The corresponding densities ρ of $80GeS_2–20Ga_2S_3$, $82GeS_2–18Ga_2S_3$, $84GeS_2–16Ga_2S_3$ glasses were 2.932, 2.905 and 2.896 g/cm^3, respectively.

The PAL spectra were performed with conventional ORTEC system of 230 ps resolution (the full width at half maximum FWHM of a single Gaussian determined by measuring ^{60}Co isotope) at the temperature T = 22 ^oC and relative humidity RH = 35 %. Contribution intensity of source is 18 %. Two identical ChG samples were used to build a characteristic sandwich arrangement needed for PAL measurements. Each PAL spectrum had been measured with a channel width of 6.15 ps (with the number of channels set to 8000) and contained no less 10^6 coincidences in total, which can be considered as conditions of improved measurement statistics. Isotope ^{22}Na of slow activity (~50 kBq) was used as source of positrons (prepared from of $^{22}NaCl$, wrapped with Kapton foil (DuPontTM, Circleville, OH) of 12 μm thickness and sealed), which was sandwiched between two identical tested samples [40,41].

The measured PAL spectra of ChG were processed with standard LT computer program [42], in which the obtained curves were fitted by two non-fixed components (τ_1, τ_2 lifetimes and I_1, I_2 intensities). Therefore, the positron trapping modes in the studied ChG, such as average positron lifetimes τ_{av}, positron lifetime in defect-free bulk τ_b and positron trapping rate in defects κ_d were calculated using a formalism of two-states trapping model [43]. The $(\tau_2 - \tau_b)$ difference was accepted as a size measure for extended free-volume defects where positrons are trapped (in terms of equivalent number of monovacancies), while τ_2/τ_b ratio was taken in a direct correlation to the nature of these defects [40]. The resulting inaccuracies in positron lifetimes τ and intensities I were ±0.003 ns and ±1 %, respectively, which led to ±0.01 ns^{-1} error-bar in positron trapping rate of defects κ_d.

DBAR measurements were performed using a Ge-detector with a resolution of 1.54 keV at 511 keV calibrated with set of standard sources (isotopes of ^{214}Pb and ^{214}Bi). Shape of 511

keV annihilation line was considered in terms of the so-called *S* and *W* parameters. The S-parameter (defined as a ratio in the central part to the total area of the annihilation line), characterizes the annihilation of positrons by low-momentum valence electrons that are sensitive to free volume defects. The *W*-parameter (defined as a ratio in the wing parts to the total area of the annihilation line) corresponds to the annihilation of positrons by high-momentum core electrons that are sensitive to the chemical environment at the annihilation site. For the DBAL spectrum the *S*-*W* parameterization energy range was selected from 502.29 to 519.71 keV (ΔS = 511 ±0.737 keV, ΔW = 511 ± [2.546÷6.36] keV), which corresponds to 260 measurement channels, giving thus an overall resolution of 0.067 keV per channel. Two independent measurements consisting of ~2×10^6 counts were performed for each sample to reproduce the analyzed DBAL spectrum. The relative errors in *S* and *W* parameters determined under such measuring protocol (when studied samples affected by different thermal treatments were removed from apparatus during measurement or principally different samples were probed) were determined to be 0.3 and 1.5 %, respectively. Since S parameter was chosen close to a reference value of ~0.5 in DBAL measurements, it could not be determined better accuracy than ±0.0015. The accuracy of determining the parameter *W* was ±0.0002.

3. Results and discussion

PAL spectrum for ChG on example of the basic $80GeSe_2$-$20Ga_2Se_3$ glasses decomposed in two components is shown in **Figure 1**.

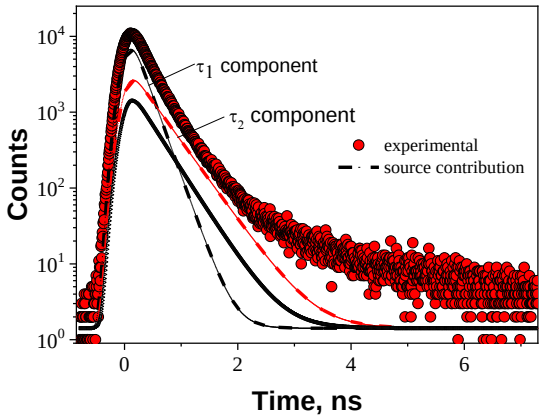

Figure 1. PAL spectrum for the basic $80GeSe_2$-$20Ga_2Se_3$ ChG decomposed on two components

Dependences of lifetimes τ_1 and τ_2 as well as intensities I_1 and I_2 on the isothermal annealin duration of the $80GeSe_2$-$20Ga_2Se_3$ glasses are presented in **Figure 2**. As noted earlier [40],

two components in the fit of experimental PAL spectra can be obtained with reduced bulk positron lifetime τ_1 which itself has no physical meaning, positron lifetime in free-volume entities (positron traps) τ_2 and corresponding intensities I_1 and I_2.

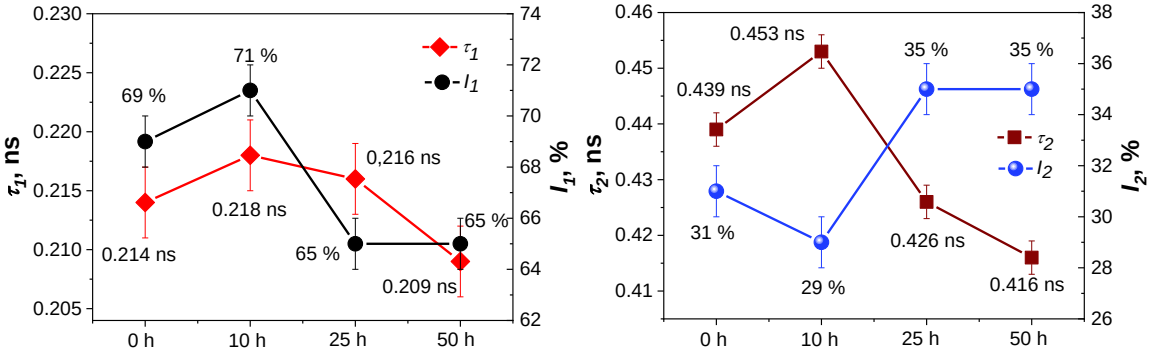

Figure 2. Dependences of lifetimes τ_1 and τ_2 as well as intensities I_1 and I_2 on annealing duration of the $80GeSe_2$-$20Ga_2Se_3$ glasses

Since (τ_1, I_1) component has no plausible physical meaning within accepted two-state positron trapping model, we will focus our further analysis on second defect-related (τ_2, I_2) component. As the annealing duration increases from the base $80GeSe_2$-$20Ga_2Se_3$ glass to the samples annealed for 10 h, the lifetime τ_2 goes up and the intensity drops, which indicates the agglomeration of voids in the material. As can be clearly seen from **Figure 3**, such tendencies lead to a decrease in positron trapping rate in defects κ_d.

However, both $\tau_{av.}$ and τ_b lifetimes remain practically unchanged (**Figure 3**). With a further increase in the duration of glass annealing to 25 h and up to 50 h, I_2 intensity begins to increase and the τ_2 lifetime decreases to 0.426 ns and 0.416 ns, respectively. Such changes lead to an increase in the κ_d. The other positron capture parameter, which is τ_2/τ_b ratio (describing the nature of defects) changes according to the parameters of the second component (**Figure 3**). However, the difference $(\tau_2 - \tau_b)$, which reflects the average size of defects where positrons are captured, naturally decreases during annealing.

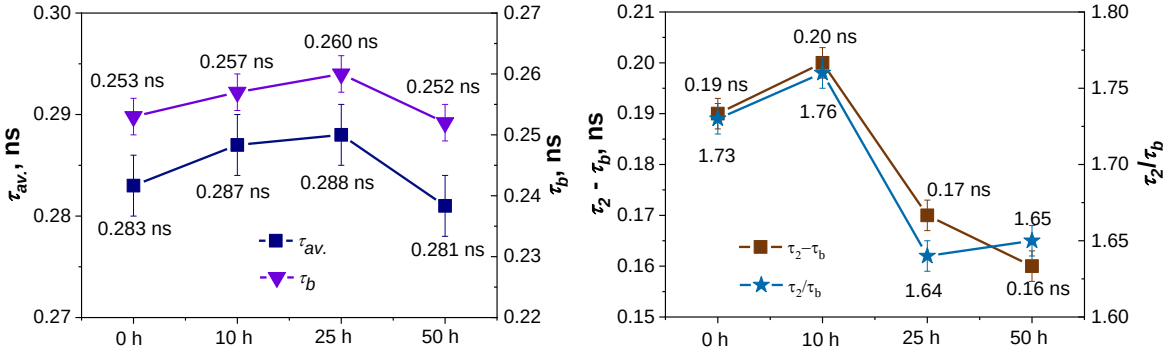

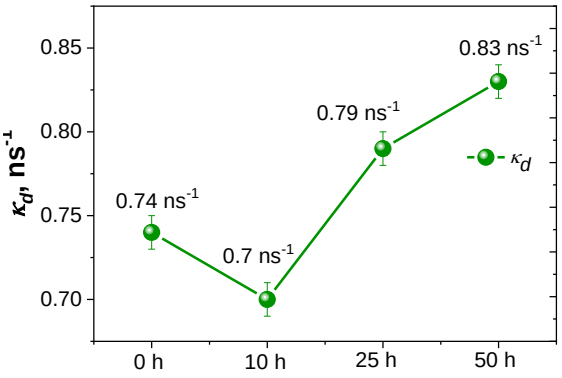

Figure 3. Dependences of positron trapping parameters on annealing duration of the $80GeSe_2$-$20Ga_2Se_3$ glasses

As was shown in [40], during annealing the structure of glasses relaxes to a thermodynamically more favorable state (crystallization shrinkage or compaction occurs), thus eliminating the excess defect-related free volumes. Such changes indicate the disappearance of existing voids or their transformation into a larger number of smaller ones. In other words, it can be argued that the crystallization of the $80GeSe_2$-$20Ga_2Se_3$ glasses due to thermal annealing at 25 h leads to the appearance of small free-volume defects due to intensive fragmentation of larger ones. Such processes accompanied by a decrease in the τ_2 lifetime and a corresponding increase in the I_2 intensity are called fragmentation. Further annealing for 50 h results in shrinkage of fragmented free-volume defects. At that, the τ_2 lifetime continues to decline but I_2 intensity does not change. Schematically, the processes of transformation of free-volume defects in the $80GeSe_2$-$20Ga_2Se_3$ ChG during crystallization (annealing at different durations) are shown in **Figure 4**.

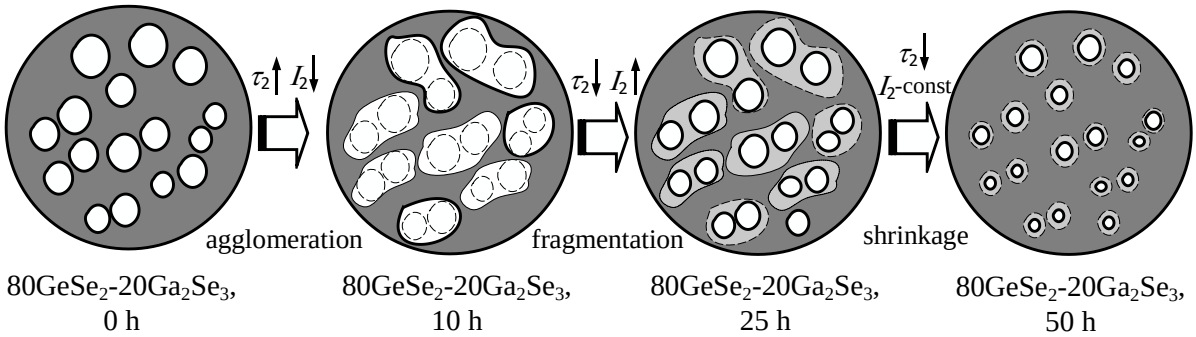

Figure 4. Processes transformation of free-volume defects in the $80GeSe_2$-$20Ga_2Se_3$ ChG during annealing

In contrast to the positron trapping parameters of the second component of PAL spectra for the annealed $80GeSe_2$-$20Ga_2Se_3$ ChG, more pronounced are changes in the positron trapping rate in defects κ_d, especially with prolonged annealing (>25 h), when specific fragmentation shows a decrease in free-volume defects with a simultaneous increase of their amount (**Figure 3**). However, the ratio τ_2/τ_b is close to 1.7 for all samples independent of their annealing duration, indicating the same type of positron trapping centers.

PAL results are fairly consistent with the DRAL studies presented in the form of correlations of *S*-*W* parameters (**Figure 5**). All points on the dependence are grouped and located close to linear trajectory, which goes towards the direction of decreasing *S* and increasing *W* for non-annealed $80GeSe_2$-$20Ga_2Se_3$ glass and for the one annealed during 10 and 25 h. This behavior reflects a so-called normal trend in changing of *S*-*W* parameters in the κ_d-ρ correlation [44] and demonstrates the agglomeration of free-volume defects in the initial stages of thermal annealing of glasses for 10 h with future fragmentation in ChG annealed at 25 h. At increase of annealing duration for 50 h, the evolution of *S*-*W* parameters changes to the opposite trend (abnormal tendency in the κ_d-ρ correlation), which reflects the shrinkage defect-related free volumes.

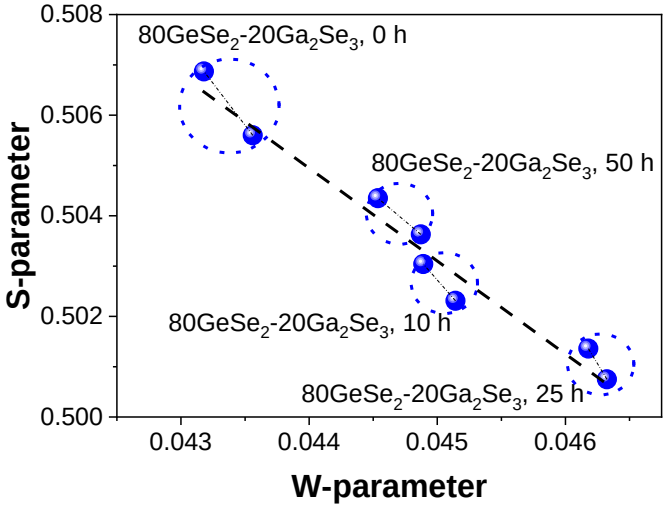

Figure 5. *S*-*W* plot for the basic and annealed $80GeSe_2$-$20Ga_2Se_3$ ChG

The dependences of positron lifetimes τ_1 and τ_2, intensities I_1 and I_2 obtained by decomposing of PAL spectrum into two components for basic GeS_2-Ga_2S_3 ChG with different content of GeS_2 and Ga_2S_3 are shown in **Figure 6**.

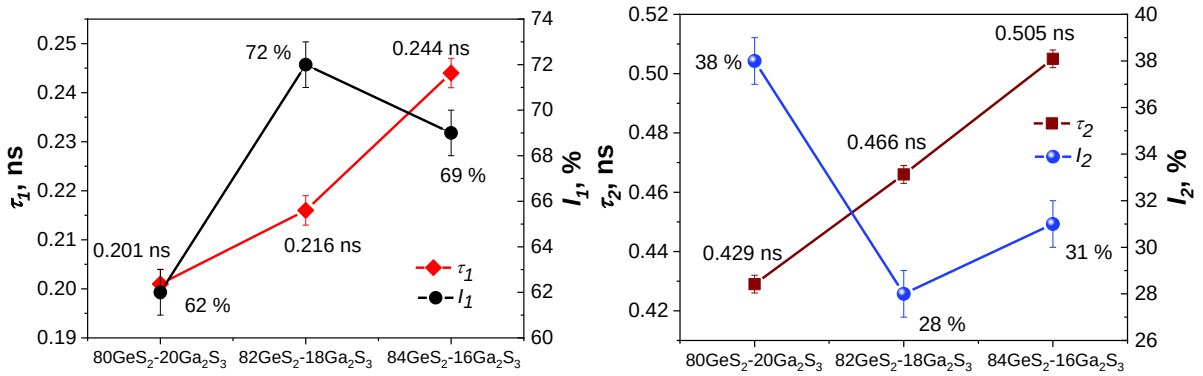

Figure 6. Dependences of lifetimes τ_1 and τ_2, intensities I_1 and I_2 for the base GeS_2-Ga_2S_3 ChG

It can be seen that the lifetime of the second component τ_2 reflects a significant increase from 0.429 ns in the $80GeS_2$-$20Ga_2S_3$ ChG to 0.505 ns in the $84GeS_2$-$16Ga_2S_3$ glasses, while the I_2 intensity decreases from 0.38 to 0.28 and increases slightly to 0.31 (**Figure 6**). The change in the ChG composition from $80GeS_2$-$20Ga_2S_3$ to $82GeS_2$-$18Ga_2S_3$ leads to agglomeration of free-volume defects with their subsequent expansion in $84GeS_2$-$16Ga_2S_3$ glasses (**Figure 7**).

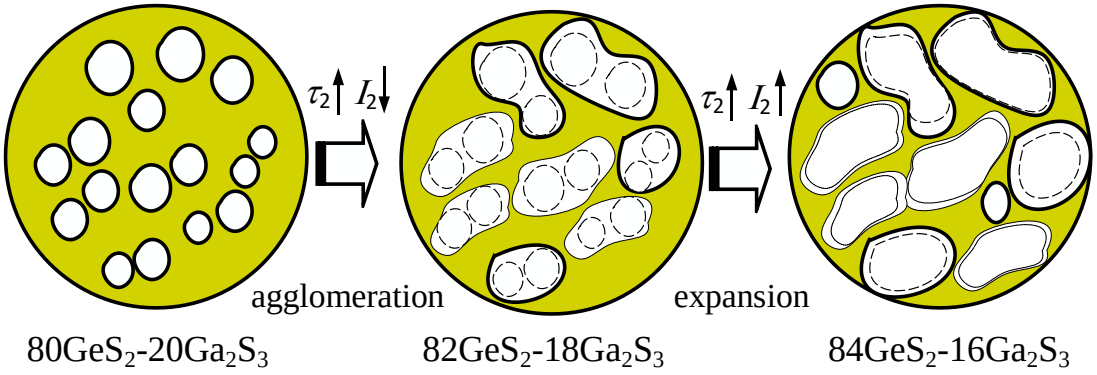

Figure 7. Transformation of free-volume defects in basic GeS_2-$20Ga_2S_3$ ChG

The observed changes in the positron trapping rate in defects κ_d are mainly associated with a decrease in the I_2 intensity (**Figure 8**). When the Ge- and Ga-containing components change, the role of internal structural states increases, and the value of κ_d parameter decreases to 0.66 ns^{-1}. Changes of the τ_b and $\tau_{av.}$ lifetimes correlate with positron trapping parameters (**Figure 8**). The nature of free-volume defects, where positrons are captured, is typical for all compositions.

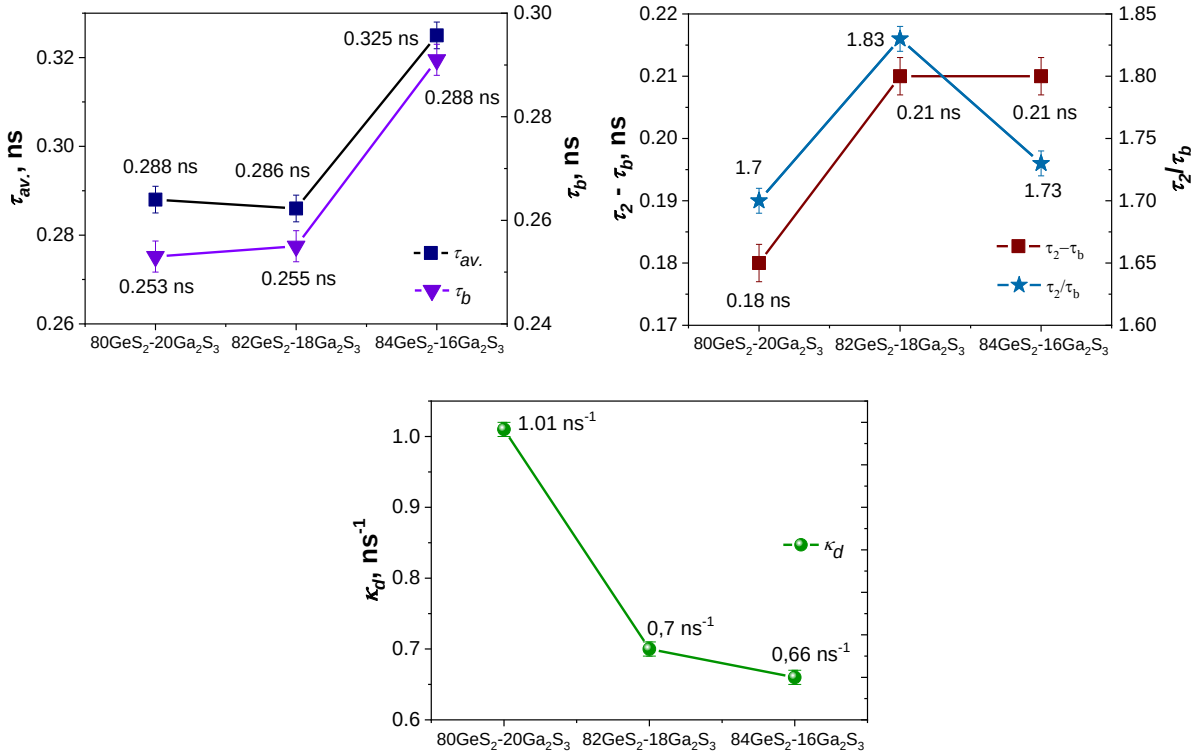

Figure 8. Dependences of positron trapping parameters for the basic GeS_2-Ga_2S_3 ChG

DRAL investigations were performed by double measurements (two points are circled in **Figure 9**). Despite only three compositions of ChG have been studied, it is difficult to draw an unambiguous conclusion about the linearity of the evolution of *S*-*W* parameters, but it can be argued that it is close to linear.

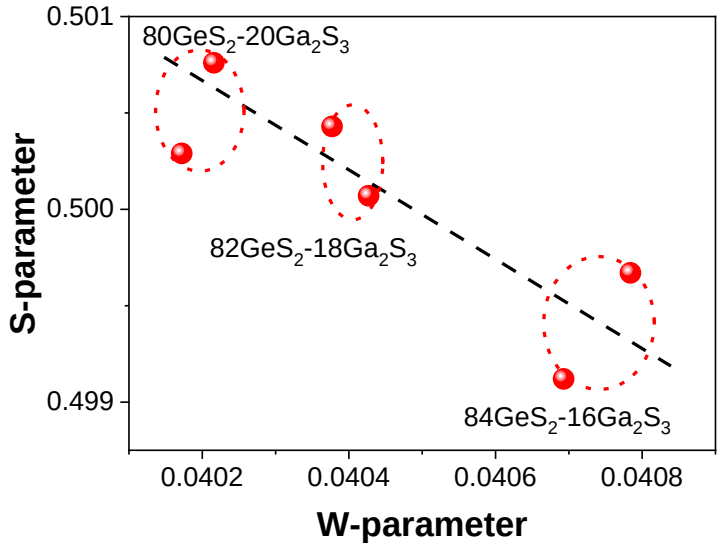

Figure 9. *S*-*W* plot for the basic GeS_2-Ga_2S_3 ChG

Thus, the grouped points of double measurements on the correlation dependence of *S*-*W* parameters are on one line from the $80GeS_2$-$20Ga_2S_3$ to $82GeS_2$-$18Ga_2S_3$ and up to $84GeS_2$-$16Ga_2S_3$ composition in the direction of decrease of *S* parameter and increase of *W* parameter. Such behavior corresponds to a so-called abnormal tendency in the κ_d-ρ correlation [41], when all defect-related components, corresponding trapping parameters and densities exhibit obvious deviations, which can be ascribed to some changes in the defect environment.

The approach considered in this work can be particularly useful for analyzing extended defect structures formed in the near-surface region of crystalline samples irradiated with fast heavy ions [45-49] or electrochemical etching [50].

4. Conclusion

Structural evolution of free-volume defects (positron trapping voids) in the Ge-Ga-S/Se chalcogenide glasses were studied on the example of the $80GeSe_2$-$20Ga_2Se_3$ glasses annealed for 10 h, 25 h and 50 h as well as the basic $80GeS_2$-$20Ga_2S_3$, $82GeS_2$-$18Ga_2S_3$ and $84GeS_2$-$16Ga_2S_3$ matrices. It is established that in the investigated ChG, two main tendencies in evolution of free-volume defect can be possible: void agglomeration and void fragmentation. Specific agglomeration of smaller voids into larger entities reveals an increase of τ_2 lifetime and decrease of I_2 intensity. Other positron trapping parameters are in correlation with components input within two-state positron trapping model.

It is shown that initial annealing of the $80GeSe_2$-$20Ga_2Se_3$ for 10 h results in agglomeration of free-volume defects with their further agglomeration at annealing for 25 h. At the final stage (annealing during 50 h) the shrinkage of fragmented voids is observed. It is shown that Ga-related free-volume sub-system plays a decisive role in positron trapping process in the GeS_2-Ga_2S_3 glasses, while the overall density variation is defined mainly by Ge-related sub-system. These results serve as basis for new characterization route for inner free-volume structure of these glasses. It can be assumed that the void agglomeration is related with increase of GeS_2 and decrease of Ga_2S_3 content (from $80GeS_2$-$20Ga_2S_3$ to $82GeS_2$-$18Ga_2S_3$). Further expansion of defect-related positron trapping sites is due to transformation to the $84GeS_2$-$16Ga_2S_3$ matrix.

Acknowledgements

HK would like to thanks Ministry of Education and Science of Ukraine (project No. 0122U000807) as well as Dr. A. Ingram for assistance in PAL and DRAL experiments an Prof. O. Shpotyuk for fruitful discussions. In addition, the research of AIP has been supported

by the Latvian-Ukrainian Grant LV-UA/2021/5. The Institute of Solid State Physics, University of Latvia (Latvia) as the Centre of Excellence has received funding from the European Union's Horizon 2020 Framework Programme H2020-WIDESPREAD01-2016-2017-Teaming Phase2 under grant agreement No. 739508, project CAMART2.

Received:
Revised:
Published online:

References

[1] X. H. Zhang, J. L. Adam, B. Bureau, B. (2019). Chalcogenide glasses. *Springer Handbook of Glass* **2017**, 525.

[2] A. Yang, M. Zhang, L. Li, Y. Wang, B. Zhang, Z. Yang, D. Tang, *Journal of the American Ceramic Society* **2016**, *99*(1), 12.

[3] I. Kebaili, I. Boukhris, M. S. Al-Buriahi, A. Alalawi, M. I. Sayyed, *Ceramics International* **2021**, *47*(1), 1303.

[4] J. L. Adam, L. Calvez, J. Trolès, V. Nazabal, *Journal of Applied Glass Science* **2015**, *6(3)*, 287.

[5] C. Wang, Y. H. Wang, Z. Z. Xiong, P. L. Li, L. H. Zhou, Y. Lu, Zhao Ch. R., Y.Q. Chen, X. X. Yu, *Optical Materials* **2020**, *100*, 109697.

[6] M. Hussain, S. H. A. Jaffery, A. Ali, C. D. Nguyen, S. Aftab, M. Riaz, S. Abbas, S. Hussain, Y. Seo, J. Jung, *Scientific reports* **2021**, *11(1)*, 1-8.

[7] A. A. Ahmed Simon, L. Jones, Y. Sakaguchi, H. Kunold, I. van Rooyen, M. Mitkova, *physica status solidi (b)* **2021**, *258(9)*, 2000429.

[8] G. N. Greaves, *Encyclopedia of Glass Science, Technology, History, and Culture 2021*, 1, 183.

[9] M. Ates, E. Yılmaz, M. K. Tanaydın, *Chalcogenide-Based Nanomaterials as Photocatalysts* **2021**, 307.

[10] D. C. Kaseman, S. Sen, *Journal of Non-Crystalline Solids* **2020**, 120500.

[11] J. Zheng, L. Li, H. Yin, Y. Wang, H. Zeng, J. Wei, G. Chen, *Journal of Non-Crystalline Solids* **2019**, *523*, 119606.

[12] Ivashchyshyn, F. O., Maksymych, V. M., Krushelnytska, T. D., Rybak, O. V., Seredyuk, B. O., & Tovstyuk, N. K. (2021). Biintercalate layered heterostructure: synthesis conditions and physical properties. Low Temperature Physics, 47(12), 1065-1071.

[13] N. Q. Diep, S. K. Wu, C. W. Liu, S. H. Huynh, W. C. Chou, C. M. Lin, D.Z. Zhang, C. H. Ho, *Scientific reports* **2021**, *11(1)*, 1-10.

[14] X. Lu, J. Li, L. Yang, R. Zhang, Y. Zhang, J. Ren, A. C. Galca, M. S. Gerald, F. P. Wang, *Journal of Non-Crystalline Solids* **2020,** *528*, 119757.

[15] Y. Yang, O. Ba, S. Dai, F. Chen, G. Boudebs, *Journal of Non-Crystalline Solids* **2021**, *554*, 120581.

[16] A. G. Prabhudessai, S. Balaji, K. Biswas, R. Dasgupta, P. Sarkar, K. Annapurna, *Journal of Non-Crystalline Solids* **2019**, *507*, 56.

[17] E. Zhu, Y. Liu, X. Sun, G. Yin, Q. Jiao, S. Dai, C. Lin, *Journal of Non-Crystalline Solids* **2019**, *X(1)*, 100015.

[18] S. K. Pal, N. Mehta, J. C. MacDonald, D. Sharma, *The European Physical Journal Applied Physics* **2020**, *90(3)*, 31101.

[19] Q. Fan, W. Zhang, H. Qing, J. Yang, *Principles Calculation. Materials* **2022**, *15(3)*, 971.

[20] I. Karbovnyk, J. Collins, I. Bolesta, A. Stelmashchuk, A. Kolkevych, S. Velupillai, S., H. Klym, O. Fedyshyn, S. Tymoshuk, I. Kolych, *Nanoscale research letters* **2015**, *10(1)*, 1.

[21] L. Mochalov, D. Dorosz, M. Kudryashov, A. Nezhdanov, D. Usanov, D. Gogova, S. Zelentsov, A. Boryakov, A. Mashin, *Spectrochimica Acta Part A: Molecular and Biomolecular Spectroscopy* **2018**, *193*, 258.

[22] M. V. Kurushkin, V. A. Markov, A. V. Semencha, M. D. Mikhailov, A. S. Tverjanovich, A. L. Shakhmin, T. V. Larionova, V. D. Andreeva, *International Journal of Applied Glass Science* **2018**, *9(1)*, 85.

[23] S. Jia, N. Shi, J. Shen, R. Wu, Q. Liu, Z. Song, M. Zhu, *physica status solidi (b)* **2021**, *258(7)*, 2100038.

[24] I. Procházka, *Materials Structure* **2001**, *8(2*), 55.

[25] F. Tuomisto, I. Makkonen, *Reviews of Modern Physics* **2013**, *85(4)*, 1583.

[26] K. Saarinen, P. Hautojärvi, C. Corbel, *Semiconductors and Semimetals* **1998**, *51*, 209.

[27] B. Li, V. Krsjak, J. Degmova, Z. Wang, T. Shen, H. Li, S. Sojak, V. Slugen, A. Kawasuso, *Journal of Nuclear Materials* **2020**, *535*, 152180.

[28] S. K. Sharma, P. K. Pujari, *Progress in Polymer Science* **2017**, *75*, 31.

[29] T. Stassin, R. Verbeke, A. J. Cruz, S. Rodríguez-Hermida, I. Stassen, J. Marreiros, M. Krishtab, M. Dickmann, W. Egger, I. F. J. Vankelecom, S. Furukawa, D. De Vos, D. Grosso, M. Thommes, R. Ameloot, *Advanced Materials* **2021**, *33(17*), 2006993.

[30] A. Dupasquier, G. Kögel, A. Somoza, *Acta Materialia* **2004**, *52(16*), 4707.

[31] A. Zubiaga, R. Warringham, N. Boltz, D. Cooke, P. Crivelli, D. Gidley, J. Pérez-Ramírez, S. Mitchell, *Physical Chemistry Chemical Physics* **2016**, *18(13*), 9211.

[32] J. Bartoš, O. Šauša, H. Švajdlenková, I. Maťko, K. Čechová, *Journal of Non-Crystalline Solids* **2019**, *511*, 1.

[33] H. Klym, I. Hadzaman, V. Gryga, *Applied Nanoscience* **2021**, 1.

[34] P. Husband, I. Bartošová, V. Slugeň, F. A. Selim, *Journal of Physics: Conference Series* **2016**, *674(1*), 012013.

[35] J. Čížek, M. Vlček, I. Procházka, *Nuclear Instruments and Methods in Physics Research Section A: Accelerators, Spectrometers, Detectors and Associated Equipment* **2010**, *623(3*), 982.

[36] V. J. Ghosh, M. Alatalo, P. Asoka-Kumar, B. Nielsen, K. G. Lynn, A. Kruseman, P. E. Mijnarends, *Physical Review B* **2000**, *61(15*), 10092.

[37] H. Klym, A. Ingram, O. Shpotyuk, I., Karbovnyk, *Optical Materials* **2016**, *59*, 39.

[38] H. Klym, A. Ingram, O. Shpotyuk, *Materialwissenschaft und Werkstofftechnik* **2016**, *47(2-3*), 198.

[39] H. Klym, A. Ingram, O. Shpotyuk, O. Hotra, A. I. Popov, *Radiation Measurements* **2016**, *90*, 117.

[40] O. Shpotyuk, L. Calvez, E. Petracovschi, H. Klym, A. Ingram, P. Demchenko, *Journal of alloys and compounds* **2014**, *582*, 323.

[41] H. Klym, A. Ingram, O. Shpotyuk, R. Szatanik, E. Petracovschi, L. Calvez, C. Lin, *Solid State Phenomena* **2015**, *230*, 221.

[42] D. Giebel, J. Kansy, *Materials Science Forum* **2011**, *666*, 138.

[43] R. Krause-Rehberg, H. S. Leipner, Positron annihilation in semiconductors: defect studies **1999**.

[44] H. Klym, A. Ingram, O. Shpotyuk, L. Calvez, E. Petracovschi, B. Kulyk, R. Serkiz, R. Szatanik, *Nanoscale research letters* **2015**, *10(1*), 1.

[45] A. Akilbekov, A. Akylbekova, A. Usseinov, A. Kozlovskyi, Z. Baymukhanov, S. Giniyatova, A.I. Popov, A. Dauletbekova, *Nuclear Inst. Meth. Phys. Res. B* **2020**, *476*, 10.

[46] A. Akilbekov, R. Balakhayeva, M. Zdorovets, Z. Baymukhanov, F.F. Komarov, K.Karim, A.I. Popov, A. Dauletbekova, *Nuclear Inst. Meth. Phys. Res. B* **2020**, *481*, 30.

[47] I. Z. Zhumatayeva, I. E. Kenzhina, A. L. Kozlovskiy, M. V. Zdorovets, *J. Mater. Sci. Mater. Electron.* **2020**, *31*, 6764.

[48] A. Kozlovskiy, D. Shlimas, I. Kenzhina, M. Zdorovets, *Mater. Res. Express* **2019**, *6*, 055026.

[49] M. Zdorovets, K. Dukenbayev, A. Kozlovskiy, I. Kenzhina, *Ceramics International* **2019**, *45*, 8130.

[50] Y. O. Sychikova, I. T. Bogdanov, S. S. Kovachov, *Functional Materials* **2019**, *27*, 29.

Free-volume extended defects in structurally-modified Ge-Ga-S/Se glasses

Transformation of free-volume extended defects in the $80GeSe_2$-$20Ga_2Se_3$ chalcogenide glasses caused by thermal annealing for 10, 25 and 50 h as well as in the GeS_2-Ga_2S_3 glasses with different GeS_2 and Ga_2S_3 contents were studied. It is shown that in the $80GeSe_2$-$20Ga_2Se_3$ glasses agglomeration of free volumes in the initial stage of annealing with further fragmentation and shrinkage is observed. Increase content of Ge-related sub-system in the GeS_2-Ga_2S_3-based glasses results in agglomeration of defects with their further expansion.

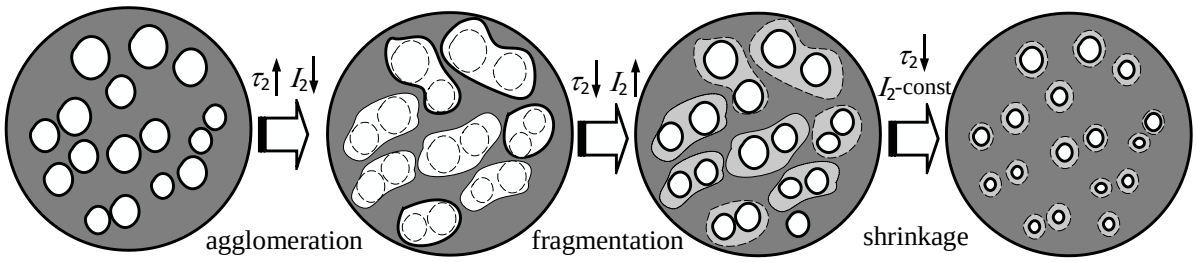

Processes transformation of free-volume defects in the $80GeSe_2$-$20Ga_2Se_3$ ChG during annealing

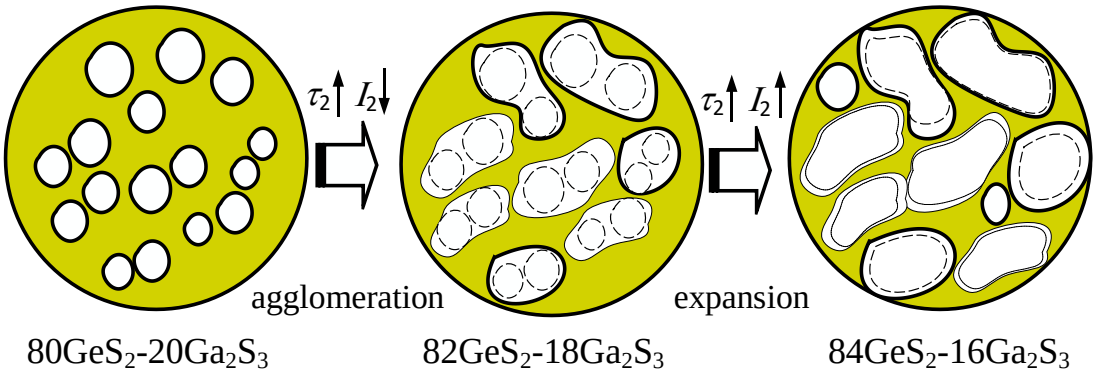

Transformation of free-volume defects in basic GeS_2-$20Ga_2S_3$ ChG